Skeletal Radiol (2013) 42:1507–1513
DOI 10.1007/s00256-013-1692-6

SCIENTIFIC ARTICLE

Total ankle arthroplasty: optimizing computed tomography imaging protocol

Ia Kohonen · Helka Koivu · Tero Vahlberg · Heli Larjava · Kimmo Mattila

Received: 26 March 2013 / Revised: 24 June 2013 / Accepted: 1 July 2013 / Published online: 3 August 2013

Abstract
Objective To evaluate parameters and positioning when imaging total ankle prostheses on computed tomography (CT).
Materials and methods An ankle prosthesis implanted into a pig's knee joint underwent 16 different CT imaging protocols. Four defects were drilled around prosthesis components simulating periprosthetic osteolytic lesions. The specimen with the implant was imaged in four different orientations with the tibial stem parallel to the table and at 25, 45, and 90° angles to it. The protocol consisted of scanning at 100, 120, and 140 kVp in every position with a pitch of 1.2. The scanning at 120 kVp in every position was repeated with a pitch of 1.0.
Results CT proved to be a reliable imaging modality when studying periprosthetic lesions adjacent to the ankle prosthesis when the tibial stem alignment was parallel to the table. When imaging at higher angles, metal artifacts distorted the image, making the analysis of periprosthetic bone structure unreliable. There were no statistically significant differences between different tube voltages or pitch in volume measurements of the osteolytic lesions.
Conclusions CT is a reliable imaging method to evaluate periprosthetic bone structure around ankle prostheses when orientation of the prosthesis and acquisition parameters is optimized.

Keywords Computed tomography · Metal artifact · Total ankle arthroplasty

I. Kohonen (✉) · K. Mattila
Medical Imaging Centre of Southwest Finland, Turku University Hospital, Kiinamyllynkatu 4-8, 20520 Turku, Finland
e-mail: ia.kohonen@tyks.fi

K. Mattila
e-mail: kimmo.mattila@tyks.fi

I. Kohonen · H. Koivu · K. Mattila
University of Turku, Turku, Finland

H. Koivu
e-mail: helka.koivu@tyks.fi

H. Koivu
Department of Internal Medicine, Rheumaortopaedic Unit, Turku University Hospital, Paimio Hospital, Preitila, Finland

T. Vahlberg
Department of Biostatistics, University of Turku, Turku, Finland
e-mail: tervah@utu.fi

H. Larjava
Central Finland Health Care District, Medical Imaging, Jyväskylä, Finland
e-mail: heli.larjava@ksshp.fi

Introduction

The number of patients with total joint prostheses and other metallic orthopedic implants has grown, resulting in an increased number of CT examinations with metallic implants. Demands for evaluating the bone structure around metallic implants have likewise increased. Conventional radiography has been and still is the primary imaging modality, partly because of its ease of availability and lower cost. However, cross-sectional imaging, both computed tomography (CT) and magnetic resonance imaging (MRI), is more widely used in characterizing bone and soft tissues around metallic components and even the implant itself [1–3]. Earlier imaging created metal artifacts that were so distorting that it was difficult to obtain diagnostic images. Nevertheless, attempts to reduce metal artifacts both on CT and MR imaging have been successful and in most cases evaluating bone structure even around metallic hardware is possible. The groundwork has been done predominantly using hip arthroplasty as a model [4–7].

Several techniques to decrease metal artifacts on CT images have been described in the literature. Acquisition as well as image reconstruction parameters affect the amount of metal artifacts that are produced. There are also newer metal artifact reduction (MAR) image reconstruction algorithms such as iterative reconstruction, projection interpolation, and adaptative filtering methods. Thus far, these methods are not

so commonly used in clinical practice; also the benefits of these reconstruction programs are somewhat controversial [8–10]. Dual-energy CT (DECT) is a promising new technique in musculoskeletal imaging and its usage in minimizing metal artifacts on images needs to be further studied [11].

Total ankle arthroplasty (TAA) is increasingly used in the treatment of painful ankle arthritis [12, 13]. Although the longevity of a total ankle replacement has improved [12], there are still concerns related to these implants. Periprosthetic osteolysis is one of the most important complications related to TAA [13–19]. Because osteolysis is typically progressive and in many cases gradually leads to component failure, it is important to evaluate the bone structure around the prosthetic components [20, 21]. There is evidence supporting CT's superiority to radiographs in detecting osteolysis-related pathology [3, 7, 20, 22].

The purpose of this study was to evaluate the effect of orientation of TAA during scanning on CT to minimize metal artifacts around prosthesis components. We also wanted to determine how imaging parameters, tube voltage, and pitch, affect the ability to characterize bone structure around total ankle prosthesis.

Materials and methods

We used AES ankle prosthesis (Ankle Evolutive System, manufactured by Transystème, Nimes, distributed by Biomet, Valence, France) in a pig's knee joint as a model. The AES total ankle prosthesis is a three-piece uncemented, unconstrained design with tibial and talar components of cobalt-chrome (Co-Cr). It has a front-to-back mobile bearing of ArCom compression molded polyethylene (Biomet, UK) between the flat tibial component and the shallow sulcus of the talar implant. We used a dissected pig's knee joint as a model because its size corresponds well to the human ankle. An orthopedic surgeon (HK) experienced in ankle arthroplasty performed the surgery. Soft tissues and skin were left around the joint. To improve the fit of the prosthetic components, the bones of the knee joint were turned "upside down" so that the talar component was placed in the femoral trochlea and the tibial component in the proximal head of tibia (Fig. 1). Additionally, four different-sized defects were drilled around the prosthetic components, simulating periprosthetic osteolytic lesions. Two defects, one large and one small, were placed around both the tibial and the talar components. Sizes of these defects were measured by filling the defects with water using a 1-ml syringe. Sizes of the defects around the tibial component were 0.55 and 2.1 ml and the talar component 0.5 and 1.5 ml. At the time of CT scanning, the defects were filled with low-fat ground meat (percentage of fat under 10 %) to simulate granuloma and avoid air in them.

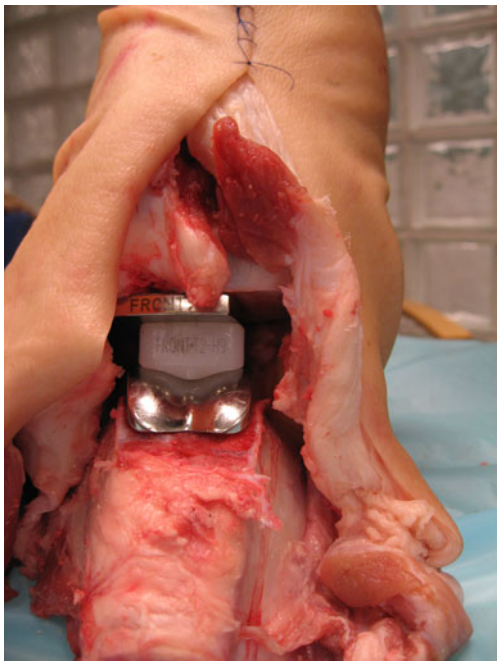

Fig. 1 Photograph of AES prosthesis in pig's knee joint

Computed tomography was performed using a Siemens Somatom Sensation 64-slice CT (Siemens AG Healthcare Sector, Erlangen, Germany). The joint with prosthesis was imaged in four different orientations: the tibial stem parallel to the table and at 25, 45, and 90° angles to it. During CT scanning, the specimen with the implant was in a cardboard box. A wooden stick was fixed to the tibial component. After that, the tibial stem could be rotated to 25, 45, and 90° angles to the table in addition to the first setting while the talar component alignment remained unchanged. The protocol consisted of scanning at 100, 120, and 140 kVp in every angle with a pitch of 1.2. The scanning at 120 kVp in every angle was repeated with a pitch of 1.0. A beam hardening and metal-artifact-minimizing algorithms were used, the latter based on the extended CT-scale technique. Also, tube current modulation was used. Since the distance of the imaged area and the thickness of the target varied according to the orientation of the tibial componet, we used cumulative tube current-time-product (mAs) to elucidate the radiation dose (Table 1). It has been calculated by adding up the mAs-values of the single slices. Table 1 also presents the values of the minimum and maximum mAs used by the automatic tube current modulation in each protocol. The slice thickness was 0.6 mm and the reconstruction increment was 0.4 mm. The streak artifacts caused by ankle prosthesis were visually appraised and the volumes of the drilled defects around prosthetic components visible on CT images were measured twice using volumetric analysis tool provided by syngo MultiModality Workplace (VE 36A, Siemens AG Healthcare Sector, Erlangen, Germany) by one radiologist (IK) with more than 5 years of experience in musculoskeletal radiology. There were approximately 11 months between the two measurement

Table 1 Imaging parameters and data in different protocols and positions. There were 16 different imaging protocols. *Angle* refers to the alignment of tibial stem to table

Angle (degrees)	kVp	Pitch	CTDIvol (CT dose volume index, mGy)	Distance imaged (cm)	mAs min	mAs max	Cumulative mAs	No of detected defects
0	100	1.2	4.81	16.8	85	115	6.023	4
0	120	1.2	8.28	16.8	83	112	5.962	4
0	120	1.0	8.27	16.8	85	113	6.070	4
0	140	1.2	12.9	16.8	77	112	5.919	4
25	100	1.2	4.88	16.8	89	116	6.032	4
25	120	1.2	8.28	16.8	90	112	5.972	4
25	120	1.0	8.27	16.8	94	113	6.037	4
25	140	1.2	12.9	16.8	92	112	5.957	4
45	100	1.2	4.81	18.9	87	114	6.748	2
45	120	1.2	8.28	18.9	86	116	6.740	2
45	120	1.0	8.16	19.2	90	116	6.789	2
45	140	1.2	12.75	19.9	88	112	6.617	2
90	100	1.2	4.29	12.3	67	115	3.909	1
90	120	1.2	7.39	12.3	65	113	3.830	1
90	120	1.0	7.51	12.6	71	111	4.107	1
90	140	1.2	12.2	12.6	72	111	4.239	2

sessions. No effort was made to keep the radiologist blinded to image parameters as interpreting the data. CT protocols are presented in Table 1.

Analysis of variance was used as a statistical method to evaluate the effect of orientation of the ankle prosthesis, the tube voltage, and the pitch on artifacts caused by the metal implant. The effects of tube voltage and angle, i.e., orientation of the tibial component, were adjusted for the component. Tukey's adjustment method was used in further pairwise comparisons in analysis of variance. Intraclass correlation between the first and second measurement sessions was calculated to test the reliability of the measurements. The limits of agreement between the first and second measurement sessions were quantified using Bland–Altman plot. Statistical analysis was performed using SAS System for Windows, version 9.2 (SAS Institute Inc., Cary, NC, USA). We used a level of significance of α=0.05.

Results

There were no significant differences between the measured and the real volumes when the tibial stem was parallel to the table with a pitch of 1.2. When the tibial stem was at 25, 45, and 90° angles to the table, there were statistically significant differences between the measurements on CT images and the real volumes (p values in all <0.0001, Table 2). Scatter plot shows the differences between the measured and real volumes according to degrees during the first measurement session (Fig. 2), the means and standard deviations (SD) were as follows: 0.02, 0.17 (0°); −0.30, 0.22 (25°); −0.52, 0.58 (45°) and −1.28, 0.26 (90°). When the tibial stem was at 45 and 90° angles to the table, the smaller defects both around the tibial and talar components could not be detected at all regardless of tube voltage because increases of artifacts caused by the implant (Fig. 3). Volume measurements with a pitch of 1.2 were significantly different between the angles (0, 25, 45, 90°) in every comparison (p<0.0125 or lower in all pairwise comparisons) except in one, between 25 and 45° (Table 3).

In the whole material with a pitch of 1.2 there were no statistically significant differences between different tube voltages (100, 120, and 140 kVp) in volume measurement differences (angle and component-adjusted p=0.24). However, when the tibial stem was at a 90° angle to the table, the larger defect around the talar component could not be detected because of gross artifacts when scanning at 100 kVp and 120 kVp (Fig. 4). Scanning at 140 kVp and in 90° angle the larger defect around the talar component could be partially identified despite the artifacts. When scanning the

Table 2 Volume measurement differences (measured volumes minus real volumes) with a pitch of 1.2. Angle means the alignment of tibial stem to table. Mean difference is tube voltage and component adjusted

Angle (degrees)	Mean difference (ml)	SE (ml)	p value*
0	0.01	0.07	0.89
25	−0.34	0.07	<0.0001
45	−0.58	0.11	<0.0001
90	−1.30	0.13	<0.0001

SE standard error

*Analysis of variance; Tukey's method was used in pairwise comparisons

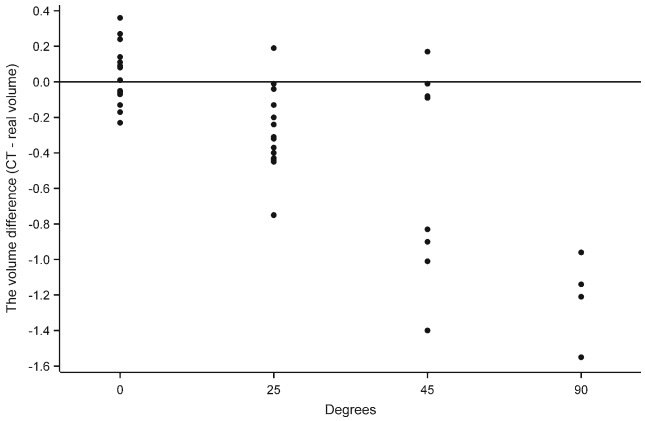

Fig. 2 Scatter plot displays the differences between the measured and real volumes (ml) according to degrees during first measurement session (0°: min −0.23, max 0.36; 25°: min −0.75, max 0.19; 45°: min −1.4, max 0.17; 90°: min −1.55, max −0.96)

ankle at 120 kVp, volume measurement differences between pitch-values 1.0 and 1.2 did not show significant differences (angle adjusted $p=0.43$). The intraclass correlation for the measurement differences between the first and second measurement sessions was 0.96, showing excellent repeatability. The limits of agreement between the first and second volume measurement session differences were from −0.28 ml to 0.28 ml (Fig. 5).

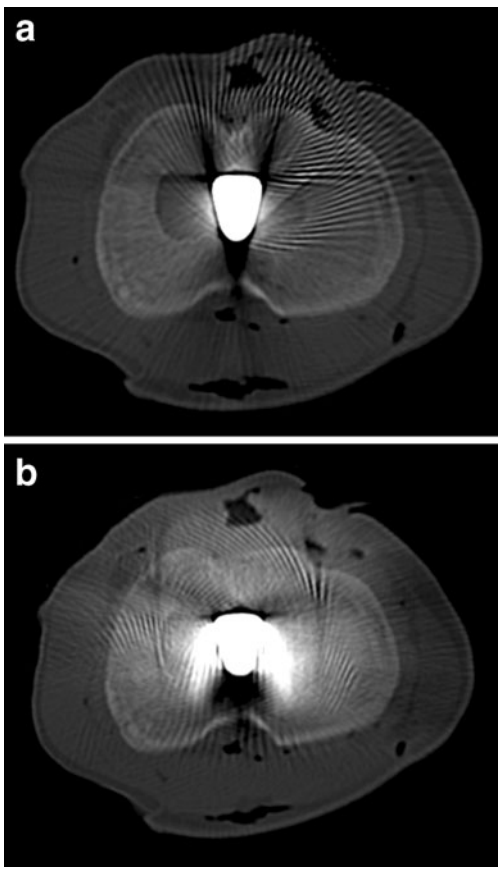

Fig. 3 Axial slices across the tibial stem. **a** On the first image (140 kV, 0°, pitch 1.2) two defects in both sides of the tibial stem are detectable. **b** On the second image (140 kV, 45°, pitch 1.2), the artifacts distort the image that only the larger defect can be detected

Table 3 Volume measurement differences (measured volumes minus real volumes) between the angles with pitch 1.2. Mean difference is tube voltage and component adjusted

Comparison	Mean difference (ml)	SE (ml)	*P* value*
0 versus 25	0.35	0.11	0.0125
0 versus 45	0.59	0.13	0.0005
0 versus 90	1.31	0.15	<0.0001
25 versus 45	0.24	0.13	0.26
25 versus 90	0.96	0.15	<0.0001
45 versus 90	0.72	0.17	0.0011

SE standard error

*Analysis of variance; Tukey's method was used in pairwise comparisons

Discussion

TAA is used more often in the treatment of damaged ankle joint instead of arthrodesis [12]. Osteolysis is one of the most important factors threatening longer-term survival of all total joint prostheses, as well as ankle prostheses [6, 15, 20, 23]. The incidence of osteolysis varies between different total ankle implant designs [14, 18, 24–26]. Traditionally, patients with total ankle prosthesis have been monitored using radiographs. However, several previous studies had shown that some periprosthetic abnormalities, e.g., osteolysis, can be detected more reliably on CT than on radiographs [4, 6, 7, 22, 27]. Therefore, we investigated the conditions to image total ankle prosthesis on CT.

All metal components cause artifacts on CT, distorting the normally excellent image quality [28, 29]. Metal composition affects the amount of artifacts produced. Titanium causes fewer artifacts than stainless steel and cobalt-chrome [7, 29, 30]. Despite the artifacts caused by the cobalt-chrome components of the ankle prosthesis in our study, CT turned out to be a reliable imaging modality when studying periprosthetic lesions around ankle prostheses in a position with the long axis of the tibial component parallel (tibial stem at 0° angle) to the table. The means and standard deviations of volume measurement differences between the measured and true values were smallest at 0° angle being in clinically acceptable limits (mean 0.02 ml, SD 0.17 ml) while in other orientations the measurement error and variance were more substantial.

The geometry of implant and cross-sectional area of it as well as the orientation of the hardware during scanning affects the artifacts produced [7, 29, 31]. Asymmetric hardware produces nonuniform artifacts [7]. These artifacts are most prominent in the direction of the hardware's greatest

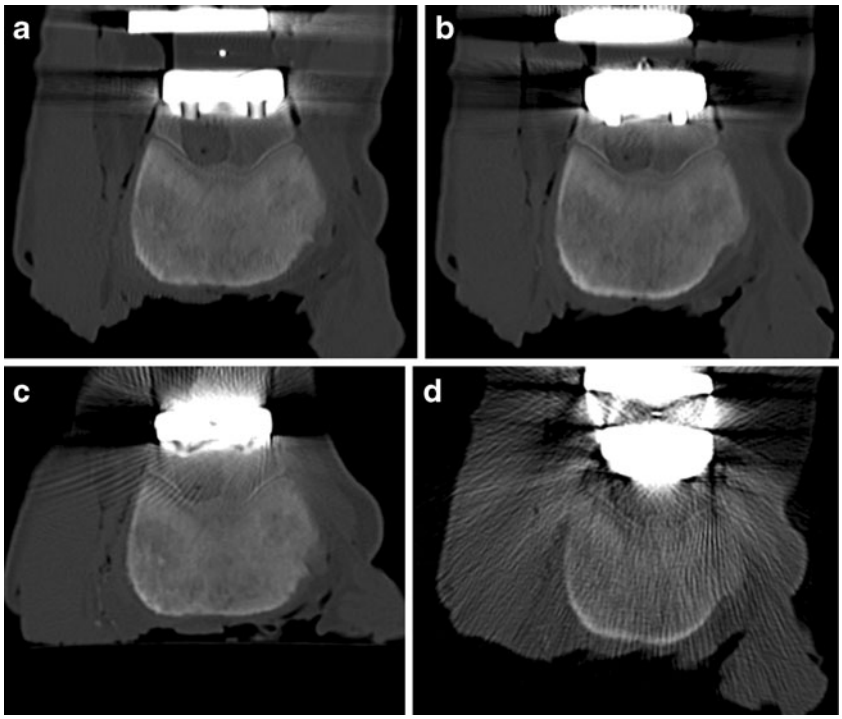

Fig. 4 Coronal slices through the larger defect under the talar component. The larger defect under the talar component is shown on images obtained with the tibial stem parallel to the table (**a**) and at 25 and 45° angles (**b**, **c**) to it. The defect is not detectable due to increasing artifacts on images obtained with the stem at a 90° angle (**d**) to the table. All images are taken with 120 kV and a pitch of 1.2

cross-sectional profile [7, 29]. In our study, there were no statistically significant differences between the volumes of periprosthetic defects measured on CT images and the real volumes when the tibial stem was parallel to the table. To achieve this position, the patient lies supine on a table with straight knees. The osteolytic lesions around the prosthetic components in the ankle appear usually above the tibial plate, around the stem, or above the edges of the plate and also below the margins of the talar component [22]. When the patient is lying supine with straight knees, the major artifacts from the tibial plate do not hide the osteolytic lesions around the tibial stem and below the talar component.

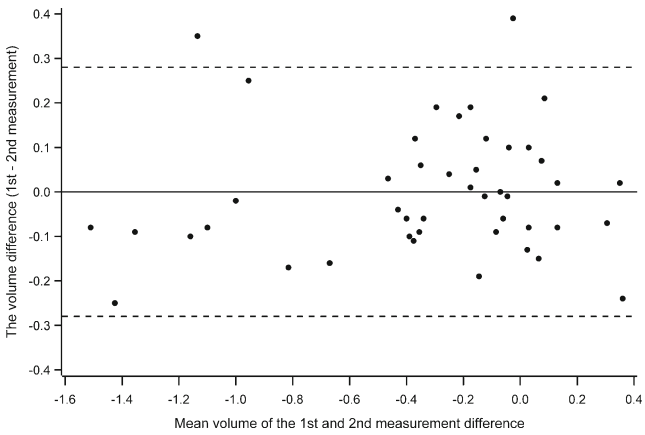

Fig. 5 Bland–Altman analysis plot. The volume differences (ml) between the 1st and 2nd measurement sessions, with *solid line* at the mean difference, and the *dotted lines* at mean difference ±1.96 × standard deviation of the volume differences (limits of agreement)

In that position, the long axis of the tibial component is perpendicular to the plane of the gantry. With higher angles, i.e., when the tibial stem was at 25, 45, and 90° angles to the table, there were statistically significant differences between the measurements on CT compared to real volumes. In many of these cases, the presence of artifacts led us to underestimate the volume of drilled defect. There were more streak artifacts on the images with tibial stem at higher angles compared to optimal positioning. Also, the orientation of the artifact lines was adverse in higher angles when considering osteolytic lesions around the TAA. Additionally, in these component orientations, the sum effect of the artifacts caused by the plate and stem may play a role. When the tibial stem was at 45 and 90° angles to the table, the smaller defects (volumes 0.55 ml and 0.5 ml) both around the tibial and talar components could not be detected at all because of gross artifacts at every studied kVp. In addition, the larger defect (volume 1.5 ml) around the talar component could not be detected when scanning at a 90° angle at 100 kVp and 120 kVp. At least part of the larger defect (volume 2.1 ml) at the tibial side could be detected in every CT protocol.

In previous studies [6, 27, 29, 32, 33], high tube voltage (140 kVp) has been used or at least recommended to obtain images with less artifacts when scanning metal hardware. Higher kilovoltage reduces noise, however it diminishes image contrast and increases radiation dose [7, 31]. In a previous study [29], a titanium alloy screw and a stainless-steel screw had been placed in a pig femur. In a comparison of CT images obtained through the short axis of the screws with two different kilovolt peaks, 140 kVp and 80 kVp, with

other parameters fixed, the higher peak voltage showed fewer artifacts. In another study, however, it was stated that there is no additional value attained when using 140 kVp tube voltage instead of 120 kVp [34]. In that study, three patients were scanned; two patients with hip prostheses (titanium and cobalt-chrome) and one patient with pelvis reconstruction using stainless-steel plates. In our study, when scanning at 140 kVp and in with a 90° angle, the bigger defects both around the tibial and talar component could be detected. However, the artifacts in that situation were so enormous that these two large defects were barely visible. There were no statistically significant differences between three different tube voltages (100, 120, and 140 kVp) in volume measurements when examining overall *p* values of the whole material. Supposing that the ankle prosthesis is in optimal orientation, i.e., the tibial stem parallel to the table, 100 kVp proved to be sufficient to evaluate periprosthetic bone structure around ankle prosthesis according to our study. The computed tomography dose volume index ($CTDI_{vol}$) values in this study were over twofold when increasing kVp from 100 to 140 (Table 1). Although $CTDI_{vol}$ does not represent patient dose [35], it describes the radiation output of a CT system. However, noteworthy is that the ankle is peripherally located with no radiosensitive organs in the imaged area [36]. The mean effective dose for CT scan of the ankle is 0.07 mSv, which is a little less than the dose on conventional chest radiograph, which is approximately 0.08 mSv [37]. In our study, the tube current modulation was used. Higher mAs result in more photons detected. It reduces noise, but increases radiation dose [7, 31]. The lowest cumulative mAs values were received when scanning the ankle prosthesis at a 90° angle (Table 1). The most likely reason for low values at 90° is that the distance imaged was shortest in that orientation. In other orientations, the cumulative mAs values were higher, also the distances imaged were longer. However, the differences in imaging distances and cumulative mAs values were quite diminutive in other orientations. Lowering the pitch settings has been shown to diminish artifacts [29, 38, 39]. A lower pitch setting allows the collection of redundant data, increasing the likelihood that adequate data will be gathered [30]. However, lowering the pitch increases radiation dose. We did not find statistically significant differences comparing volume measurements when using different pitches at 120 kVp. However, only two pitch values, 1 and 1.2, were studied. Comparing the first and second measurement sessions, the limits of agreement of volume measurement differences were clinically acceptable varying from −0.28 ml to 0.28 ml.

There are several limitations in this study. First, we used AES prosthesis, which is no longer commercially available because of rapidly appearing osteolysis related to that implant. However, there are other prostheses in the market with similar configurations and the same material as the AES. Secondly, we studied only one sample (one pig's knee joint) with the AES prosthesis implanted in it, so it was not possible to take account of the variation between the pig's knees in statistical models. Thirdly, it was difficult to make the analyst blinded with regard to image settings. Using the workstation available for the measurements, a radiologist can easily see the angles used at the time of imaging. There was only one analyst measuring the size of the defects on the CT scans, which is a limitation as well. Also, the amount of defects around the prosthetic components was known by the analyst and the number of detected defects was low at higher imaging angles because of gross metal artifacts distorting the image and making some of the defects undetectable. For example, when scanning with the pitch of 1.2 and all three tube voltages in a 90° angle, the combined amount of detected defects was four when the true amount of defects was 12. The number of detected periprosthetic defects in every imaging protocol is shown in Table 1. A limitation is also that we did not study the prospects of different MAR image reconstruction algorithms in decreasing metal artifacts.

In conclusion, computed tomography is a good imaging method to evaluate periprosthetic bone structure around an ankle prosthesis when orientation of the hardware and acquisition parameters are optimized. The orientation of the prosthesis seems to be critical. If it is not optimized, not even high voltages may help in obtaining sufficient image quality. When imaging implants with different configurations, the image protocol should be optimized individually; keeping in mind that the artifacts are most severe in the direction of the implant's greatest cross-sectional profile and the long axis of the prosthesis should be placed perpendicular to the plane of the gantry. The radiation dose is essentially negligible, because the ankle is peripherally located with no radiosensitive organs in the imaged area.

Acknowledgments Nina Heikkinen, radiographer, is acknowledged for performing CT scans.

Conflict of interest The authors declare that they have no conflicts of interest.

References

1. Buckwalter KA, Lin C, Ford JM. Managing postoperative artifacts on computed tomography and magnetic resonance imaging. Semin Musculoskelet Radiol. 2011;15:309–19.
2. Ohashi K, El-Khoury GY, Bennett DL, Restrepo JM, Berbaum KS. Orthopedic hardware complications diagnosed with multi-detector row CT. Radiology. 2005;237:570–7.
3. Sofka CM, Potter HG, Adler RS, Pavlov H. Musculoskeletal imaging update: current applications of advanced imaging techniques to evaluate the early and long-term complications of patients with orthopedic implants. HSS J. 2006;2:73–7.

4. Cahir JG, Toms AP, Marshall TJ, Wimhurst J, Nolan J. CT and MRI of hip arthroplasty. Clin Radiol. 2007;62:1163–71.
5. Hayter CL, Potter HG, Su EP. Imaging of metal-on-metal hip resurfacing. Orthop Clin North Am. 2011;42:195–205.
6. Puri L, Wixson RL, Stern SH, Kohli J, Hendrix RW, Stulberg SD. Use of helical computed tomography for the assessment of acetabular osteolysis after total hip arthroplasty. J Bone Joint Surg Am. 2002;84:609–14.
7. Roth TD, Maertz NA, Parr JA, Buckwalter KA, Choplin RH. CT of the hip prosthesis: appearance of components, fixation, and complications. Radiographics. 2012;32:1089–107.
8. Liu PT, Pavlicek WP, Peter MB, Spangehl MJ, Roberts CC, Paden RG. Metal artifact reduction image reconstruction algorithm for CT of implanted metal orthopedic devices: a work in progress. Skeletal Radiol. 2009;38:797–802.
9. Malan DF, Botha CP, Kraaij G, Joemai RM, van der Heide HJ, Nelissen RG, et al. Measuring femoral lesions despite CT metal artefacts: a cadaveric study. Skeletal Radiol. 2012;41:547–55.
10. Watzke O, Kalender WA. A pragmatic approach to metal artifact reduction in CT: merging of metal artifact reduced images. Eur Radiol. 2004;14:849–56.
11. Nicolaou S, Liang T, Murphy DT, Korzan JR, Ouellette H, Munk P. Dual-energy CT: a promising new technique for assessment of the musculoskeletal system. Am J Roentgenol. 2012;199:78–86.
12. Gougoulias N, Khanna A, Maffulli N. How successful are current ankle replacements?: a systematic review of the literature. Clin Orthop Relat Res. 2010;468:199–208.
13. Krause FG, Windolf M, Bora B, Penner MJ, Wing KJ, Younger AS. Impact of complications in total ankle replacement and ankle arthrodesis analyzed with a validated outcome measurement. J Bone Joint Surg Am. 2011;93:830–9.
14. Besse JL, Brito N, Lienhart C. Clinical evaluation and radiographic assessment of bone lysis of the AES total ankle replacement. Foot Ankle Int. 2009;30:964–75.
15. Koivu H, Kohonen I, Sipola E, Alanen K, Vahlberg T, Tiusanen H. Severe periprosthetic osteolytic lesions after the Ankle Evolutive System total ankle replacement. J Bone Joint Surg Br. 2009;91:907–14.
16. Kokkonen A, Ikavalko M, Tiihonen R, Kautiainen H, Belt EA. High rate of osteolytic lesions in medium-term follow-up after the AES total ankle replacement. Foot Ankle Int. 2011;32:168–75.
17. Knecht SI, Estin M, Callaghan JJ, Zimmerman MB, Alliman KJ, Alvine FG, et al. The Agility total ankle arthroplasty. Seven to sixteen-year follow-up. J Bone Joint Surg Am. 2004;86:1161–71.
18. Rodriguez D, Bevernage BD, Maldague P, Deleu PA, Tribak K, Leemrijse T. Medium term follow-up of the AES ankle prosthesis: high rate of asymptomatic osteolysis. Foot Ankle Surg. 2010;16:54–60.
19. Roukis TS. Incidence of revision after primary implantation of the Agility total ankle replacement system: a systematic review. J Foot Ankle Surg. 2012;51:198–204.
20. Beck RT, Illingworth KD, Saleh KJ. Review of periprosthetic osteolysis in total joint arthroplasty: an emphasis on host factors and future directions. J Orthop Res. 2012;30:541–6.
21. Lavernia CJ. Cost-effectiveness of early surgical intervention in silent osteolysis. J Arthroplasty. 1998;13:277–9.
22. Kohonen I, Koivu H, Pudas T, Tiusanen H, Vahlberg T, Mattila K. Does computed tomography add information on radiographic analysis in detecting periprosthetic osteolysis after total ankle arthroplasty? Foot Ankle Int. 2013;34:180–8.
23. Bauer TW, Schils J. The pathology of total joint arthroplasty. II. Mechanisms of implant failure. Skeletal Radiol. 1999;28:483–97.
24. Pyevich MT, Saltzman CL, Callaghan JJ, Alvine FG. Total ankle arthroplasty: a unique design, Two to twelve-year follow-up. J Bone Joint Surg Am. 1998;80:1410–20.
25. Skytta ET, Koivu H, Eskelinen A, Ikavalko M, Paavolainen P, Remes V. Total ankle replacement: a population-based study of 515 cases from the Finnish Arthroplasty Register. Acta Orthop. 2010;81:114–8.
26. Wood PL, Deakin S. Total ankle replacement. The results in 200 ankles. J Bone Joint Surg Br. 2003;85:334–41.
27. Hanna RS, Haddad SL, Lazarus ML. Evaluation of periprosthetic lucency after total ankle arthroplasty: helical CT versus conventional radiography. Foot Ankle Int. 2007;28:921–6.
28. Barrett JF, Keat N. Artifacts in CT: recognition and avoidance. Radiographics. 2004;24:1679–91.
29. Lee MJ, Kim S, Lee SA, Song HT, Huh YM, Kim DH, et al. Overcoming artifacts from metallic orthopedic implants at high-field-strength MR imaging and multi-detector CT. Radiographics. 2007;27:791–803.
30. Stradiotti P, Curti A, Castellazzi G, Zerbi A. Metal-related artifacts in instrumented spine. Techniques for reducing artifacts in CT and MRI: state of the art. Eur Spine J. 2009;18:102–8.
31. Kataoka ML, Hochman MG, Rodriguez EK, Lin PJ, Kubo S, Raptopolous VD. A review of factors that affect artifact from metallic hardware on multi-row detector computed tomography. Curr Probl Diagn Radiol. 2010;39:125–36.
32. Douglas-Akinwande AC, Buckwalter KA, Rydberg J, Rankin JL, Choplin RH. Multichannel CT: evaluating the spine in postoperative patients with orthopedic hardware. Radiographics. 2006;26:97–110.
33. West AT, Marshall TJ, Bearcroft PW. CT of the musculoskeletal system: what is left is the days of MRI? Eur Radiol. 2009;19:152–64.
34. Haramati N, Staron RB, Mazel-Sperling K, Freeman K, Nickoloff EL, Barax C, et al. CT scans through metal scanning technique versus hardware composition. Comput Med Imaging Graph. 1994;18:429–34.
35. McCollough CH, Leng S, Yu L, Cody DD, Boone JM, McNitt-Gray MF. CT dose index and patient dose: they are not the same thing. Radiology. 2011;259:311–6.
36. Haapamaki VV, Kiuru MJ, Koskinen SK. Ankle and foot injuries: analysis of MDCT findings. Am J Roentgenol. 2004;183:615–22.
37. Biswas D, Bible JE, Bohan M, Simpson AK, Whang PG, Grauer JN. Radiation exposure from musculoskeletal computerized tomographic scans. J Bone Joint Surg Am. 2009;91:1882–9.
38. Buckwalter KA, Parr JA, Choplin RH, Capello WN. Multichannel CT imaging of orthopedic hardware and implants. Semin Musculoskelet Radiol. 2006;10:86–97.
39. Ohashi K, El-Khoury GY. Musculoskeletal CT: recent advances and current clinical applications. Radiol Clin N Am. 2009;47:387–409.